JOURNAL OF GEOPHYSICAL RESEARCH, VOL. 104, NO. D18, PAGES 22,233–22,241, SEPTEMBER 27, 1999

On shortwave radiation absorption in overcast atmospheres

K. K. Fung[1] and V. Ramaswamy

NOAA Geophysical Fluid Dynamics Laboratory, Princeton University, Princeton, New Jersey

Abstract. Using a numerical model of solar radiative transfer that is calibrated against benchmark computations, it is shown that atmospheric water vapor, together with the microphysical characteristics of water drops (liquid water path and effective radius), plays an important role in the total solar spectrum reflection and absorption in overcast skies. For any specific cloud type, the water vapor column above the cloud and the presence of saturated water vapor inside the cloud contribute significantly to atmospheric absorption. These factors also affect the relationship between the net shortwave fluxes at the top and bottom of overcast atmospheres, in particular, inhibiting a general universal linkage between these two quantities. Thus neglect of details concerning the vertical location, extent, and microphysical aspects of clouds can lead to biases in the inference of surface irradiance using top-of-the-atmosphere measurements.

1. Introduction

The radiative effects of overcast skies play an important part in the shortwave heat budget of the planet, with the solar heating of the atmosphere-surface system determining the diabatic heating and general circulation characteristics of the climate system. Two issues of particular interest in this regard are (1) the characteristics of the atmospheric absorption in the presence of clouds and water vapor and (2) the relationship prevailing between the surface and top-of-the-atmosphere (TOA) irradiances. The second item holds a special appeal inasmuch as it allows a routine estimate of the surface quantity from TOA satellite measurements provided the relationship between the parameters is a general one that is valid for all types of cloud situations [*Schmetz*, 1993; *Li et al*., 1993, 1997].

Here we use a radiative transfer model that incorporates a state-of-the-art parameterization and inquire into the quantitative roles of both cloud drops and water vapor on the reflected and absorbed fluxes in plane-parallel, horizontally homogeneous overcast atmospheres, and the accompanying effects on the net TOA-surface shortwave flux relationships. The analyses here for the total solar spectrum extends the inferences of *Ramaswamy and Freidenreich* [1998] (hereafter RF98), who performed overcast atmosphere computations for the near-infrared spectrum using a "benchmark" radiation algorithm. In particular, the results obtained in that paper with respect to cloud geometric thickness, vertical location, and water vapor are extended to the total spectrum in this investigation.

2. Model

We employ the recently formulated Geophysical Fluid Dynamics Laboratory (GFDL) shortwave radiative transfer model [*Freidenreich and Ramaswamy*, 1999]. The model has been developed on the basis of and tested against benchmark results [*Ramaswamy and Freidenreich*, 1991, 1998]. The solar spectrum is split into 25 distinct bands, and the algorithm accounts for all of the principal absorbing and scattering constituents. Aerosols are not considered in the present calculations. For any homogeneous layer and at any pseudomonochromatic frequency, the layer single-scattering properties, viz., extinction optical depth, single-scattering albedo, and asymmetry factor, are given by

$$\tau_{\text{layer}} = \tau_{\text{sc}}(\text{drop}) + \tau_{\text{abs}}(\text{drop}) + \tau(\text{H}_2\text{O}) + \tau(\text{CO}_2) + \tau(\text{O}_3) + \tau(\text{O}_2) + \tau(\text{rayleigh}) \quad (1)$$

$$\omega_{\text{layer}} = [\tau_{\text{sc}}(\text{drop}) + \tau(\text{rayleigh})]/\tau_{\text{layer}} \quad (2)$$

$$g_{\text{layer}} = \{[\tau_{\text{sc}}(\text{drop})g(\text{drop})] + [\tau(\text{rayleigh})g(\text{rayleigh})]\}/[\tau_{\text{sc}}(\text{drop}) + \tau(\text{rayleigh})], \quad (3)$$

respectively, where τ_{sc}(drop) and τ_{abs}(drop) denote the scattering and absorption optical depths of the cloud drops; $\tau(\text{H}_2\text{O})$, $\tau(\text{CO}_2)$, $\tau(\text{O}_2)$, and $\tau(\text{O}_3)$ refer to the absorption optical depths of the principal gases; and τ(rayleigh) refers to the molecular scattering optical depth. The symbol g denotes the asymmetry factor, with g(rayleigh) being 0.

The radiative transfer model has 51 layers in the vertical, separated by 20 mbar, except for the bottommost layer, which is 13 mbar thick. Multiple-scattering process is handled via the delta-Eddington formulation, with appropriate scaling of the single-scattering properties in each layer [*Joseph et al*., 1976; *Briegleb*, 1992]. The homogeneous layers are then "added" to yield the distribution of the irradiances in the vertically inhomogeneous atmosphere [*Ramaswamy and Bowen*, 1994]. Cloud optical properties are prescribed according to *Slingo* [1989]. The single-scattering properties of the clouds are represented in terms of the liquid water path (LWP) and effective radius r_{eff} of drop-size distribution as

$$\tau_{\text{ext},i}(\text{drop}) = \tau_{\text{sc},i}(\text{drop}) + \tau_{\text{abs},i}(\text{drop}) = \text{LWP}\,[a(i) + b(i)/r_{\text{eff}}] \quad (4)$$

$$1 - \omega_i(\text{drop}) = c(i) + d(i)r_{\text{eff}} \quad (5)$$

$$g_i(\text{drop}) = e(i) + f(i)r_{\text{eff}}, \quad (6)$$

[1]Temporarily at GFDL Atmospheric and Oceanic Sciences Program, Princeton University, Princeton, New Jersey.

Paper number 1999JD900457.

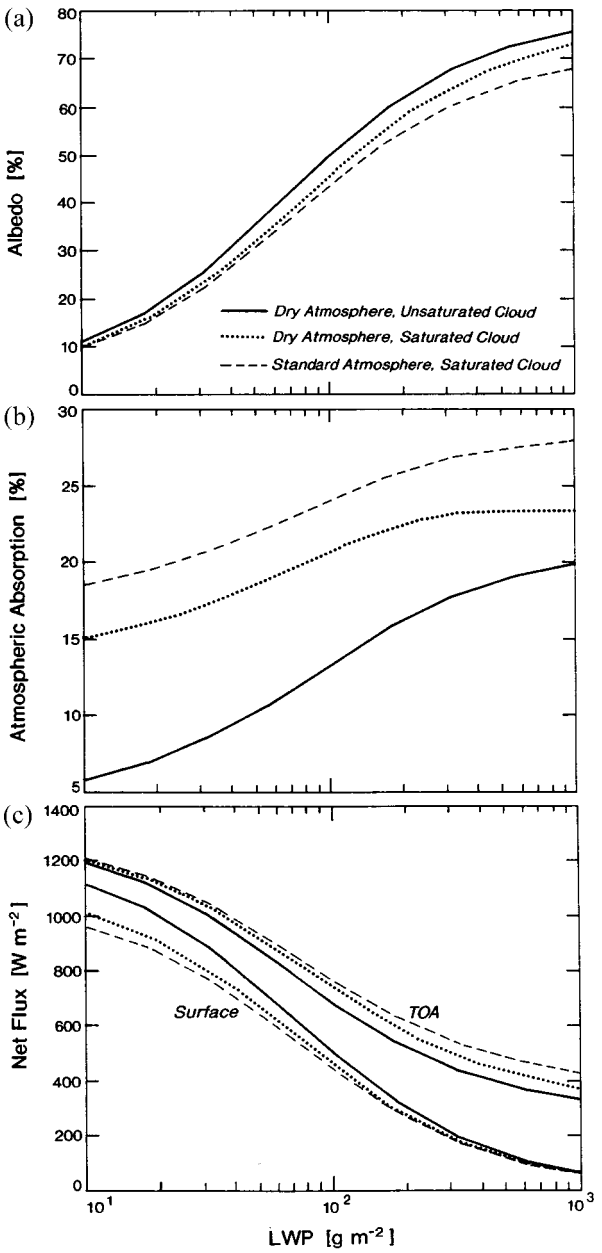

Figure 1. Percent of incident solar flux that is (a) reflected and (b) absorbed in a midlatitude atmosphere containing a cloud at 800–900 mbar, as a function of LWP. Drop effective radius is 10 μm, and overhead Sun conditions and zero surface albedo are assumed. Three different assumptions about atmospheric water vapor are considered (see section 3). Figure 1c shows net flux at the TOA and surface for the cases considered above.

where i refers to a particular wavelength interval over which the cloud drop optical properties are uniform, $\tau_{\text{ext},i}$(drop) is the cloud extinction optical depth, ω_i is the single-scatter albedo, g_i is the asymmetry parameter, and a, b, c, d, e, and f are coefficients [see *Slingo*, 1989].

We carry out a series of sensitivity calculations by varying either cloud LWP or r_{eff}, keeping the other parameters fixed. Calculations are carried out for plane-parallel, horizontally homogeneous, model single cloud systems inserted at select model altitudes in a midlatitude summer atmospheric profile [*McClatchey et al.*, 1972]. The range in LWP considered is from 10 to 1000 g/m^2, while the r_{eff} considered is 5–15 μm. In order to illustrate the role played by water vapor above and inside the cloud, we consider different assumptions related to water vapor amount in the atmosphere. The nominal (and the most realistic) case for the calculations is with a climatological profile but with the cloud layers containing water at saturation amounts corresponding to the temperature within the layer/s; we designate this as the "standard atmosphere, saturated cloud," or the nominal case. In order to delineate the role of the water vapor, we also consider two hypothetical cases. One is an entirely dry atmosphere, with water vapor mixing ratio of 3 ppmm everywhere, including inside the cloud layers; in this case, the solar radiation interacts with principally the drops, and vapor is relegated to a negligible role. We designate this as the "dry atmosphere, unsaturated cloud" case. We further consider a variation of the aforementioned case with only the cloud layer containing water at saturation value, while elsewhere the water vapor mixing ratio is 3 ppmm. Then the atmosphere outside the cloud layer becomes virtually transparent to solar radiation; this is designated as the "dry atmosphere, saturated cloud" case.

In addition to considering the aforementioned range in LWPs, we also carry out calculations for a semiinfinite cloud whose LWP is extremely large and approaches infinity. We compute the reflection and absorption of the semiinfinite cloud corresponding to different effective drop radii. The semiinfinite case provides a theoretically based asymptotic evaluation of the cloud reflection and absorption values. Virtually all of the calculations are carried out for overhead Sun; however, results for other incident Sun angles confirm the principal conclusions here. A nonreflecting surface (zero albedo) is assumed for convenience; thus the principal inferences here are applicable to low-albedo surfaces (e.g., oceans). However, one sensitivity test is carried out for a surface albedo of 0.8.

3. Dependence on Cloud and Vapor Properties

First, we consider a typical low cloud, located at 800–900 mbar and having a drop effective radius of 10 μm. We consider each of the three assumptions above concerning water vapor in the atmosphere and compute the reflected and atmospheric absorbed irradiances (or fluxes) as a function of LWP. Figure 1 illustrates the percentage of incoming solar irradiance reflected and absorbed by the surface-atmosphere system and the net irradiances at the TOA and surface.

For the LWP range from 10 to 1000 g/m^2, which is equivalent to an optical depth variation from ~1.5 to 150, the atmospheric reflectivity (or albedo) for the nominal case varies from ~10 to 70%, while the absorptivity varies from ~18% to 28%. Both reflection and absorption increase in a nonlinear manner with increase in LWP (or, equivalently, optical depth [e.g., *Stephens*, 1978]). For any LWP the quantitative differences between the three assumptions concerning water vapor highlight its role in overcast atmospheres. Relative to the dry atmosphere, unsaturated cloud layer case, the case with nominal water vapor in the atmosphere and saturated water vapor in the cloud layers enhances the atmospheric absorption by a factor of around 1.5 or more, depending on the LWP; cloud albedo is also affected nonnegligibly. Relative to a saturated cloud layer but an otherwise dry atmosphere, there is still a factor of ~1.2 enhancement of the absorption for the nominal

case. These results reiterate the findings of *Davies et al.* [1984] and *Crisp* [1997].

While the treatment above has compared somewhat idealized cases of water vapor amounts, it is useful to contrast the differences in absorption obtained above with those obtained from considerations of realistic profiles occurring in different geographic regimes. As an example, we consider the differences for the midlatitude summer (MLS), tropical (T), and sub-Arctic winter (SAW) conditions [*McClatchey et al.*, 1972], which contain 29.3, 41.3, and 4.4 kg/m^2 column water vapor amounts, respectively. For a solar zenith angle of 3° the absorption by water vapor in clear skies for T and SAW is ~1.1 and 0.55 times, respectively, that for MLS (RF98). If a typical low cloud located at 800–900 mbar with a drop optical depth of 10 is considered in each of the above atmospheres, the atmospheric absorption for the T and SAW cases is ~1.07 and 0.68 times, respectively, that for MLS (RF98). Thus differences in the water vapor amounts occurring in various geographic regions can yield significant differences in the absorbed irradiance, consistent with the inference derived from the idealized water vapor situations considered in Figure 1.

The enhancement of the absorption is also manifest in the net irradiances at TOA and surface. For the nominal case, water vapor absorption increases the net downward irradiance at the top relative to the other two cases, while at the bottom, there is a greater depletion of the irradiance reaching the surface. Note that the difference in the net irradiances between the various atmospheric water vapor assumptions is not quantitatively the same at all LWPs (differences can be as large as 100 W/m^2). The net TOA exhibits a slightly larger absolute difference between the three water vapor assumptions at the higher LWPs, while the surface irradiance exhibits larger differences at the smaller LWPs. Thus atmospheric water vapor effect for the case of low and high LWPs exerts opposing sensitivities at the top and bottom of the atmosphere. For the net TOA irradiance, at high LWPs, when the drop extinction optical depth is large, there is a difference in atmospheric absorption brought about by water vapor inside and above cloud. The presence of water vapor provides an opportunity for an enhancement of absorption of the long photon paths initiated by the drop multiple scattering; at low LWPs these path lengths are relatively short, and the difference in absorption due to the presence of vapor is much less prominent. The TOA irradiance in Figure 1c is capturing the sense of the variations in reflection seen in Figure 1a. Note that, in Figure 1a, for the nominal water vapor assumption, the differences in reflection are more pronounced at the higher LWPs. For the surface, only at the smaller LWPs would the effect of water vapor matter vis-a-vis that of the drops, while at the larger LWPs, the drops are the principal determinant of the radiation reaching the surface (RF98). Both the TOA and surface net irradiances decrease with increasing LWP, consistent with Figures 1a and 1b and with the fact that atmospheric optical thickness increases with LWP.

Next we consider the variation in reflectivity and absorptivity with respect to r_{eff}, keeping LWP fixed at 500 g/m^2. The results are illustrated in Figures 2a–2c. Only the nominal and the completely dry atmosphere cases are considered here, for convenience. From Slingo's formulation, the extinction optical depth increases with LWP but decreases with r_{eff}. Thus increase in r_{eff} implies a lesser optical depth, and thus a lesser reflection. Additionally, an increase in r_{eff} lowers the single-scattering albedo in the near infrared where drops are absorbing, resulting in greater absorption. There is likewise a slight increase in the asymmetry factor; this implies more forward scattering at each single-scattering event and contributes to a lesser reflection. Comparison of the two atmospheric water vapor assumptions again reveals significant differences in both the albedo (~7% in terms of the units plotted in Figure 2) and atmospheric absorption (about 8–10% in terms of the units plotted in Figure 2). As a consequence, the net fluxes at TOA and surface exhibit a difference between the dry and nominal water vapor cases. In contrast to Figure 1, the absolute value of the difference is fairly uniform for the range in r_{eff} considered. The variation with r_{eff} is much less nonlinear than is seen with respect to LWP (Figure 1). This is due to the fact that the optical depth varies only by a factor of 3 for the range in r_{eff} shown, whereas that shown for LWP represents a variation of

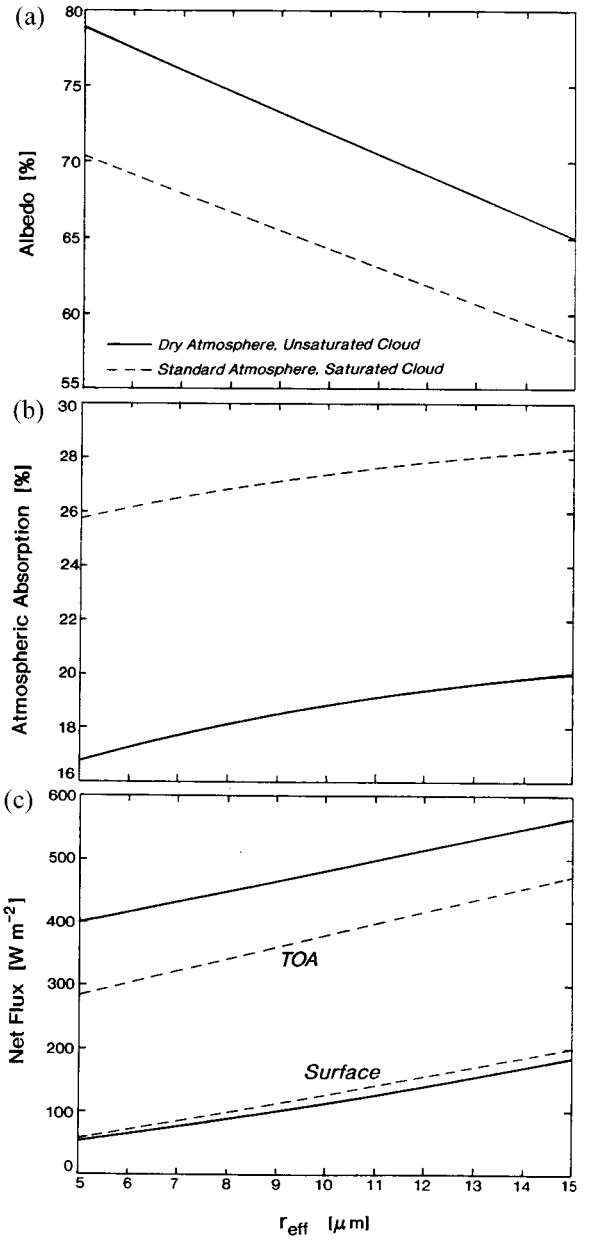

Figure 2. Same as Figure 1 except as a function of drop effective radius and for only two water vapor assumptions. LWP is held fixed at 500 g/m^2.

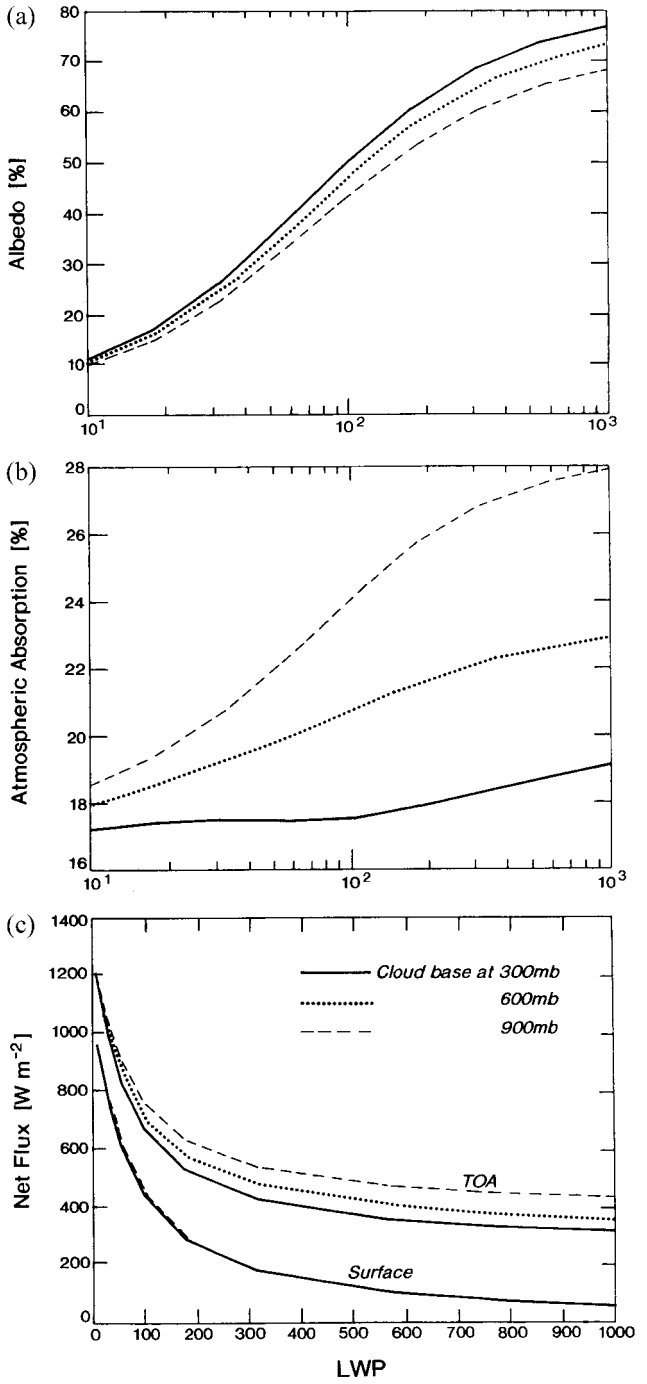

Figure 3. Same as Figure 1, except for nominal water vapor conditions and considering three different cloud systems, placed at 200–300, 500–600, and 800–900 mbar. LWP is in g/m^2.

2 orders of magnitude. The form of the curves in Figure 2 suggests that a parameterization accounting for the variation with respect to r_{eff} is relatively easier than for the case of variations with respect to LWP.

In contrast to the RF98 calculations, the above calculations include the effect of CO_2 absorption in the near infrared as well. As a measure of the role of CO_2, varying its concentration from 190 to 360 ppmv results in a negligible effect on the upward flux, while the downward flux is affected by 0.2% or less (for overhead Sun conditions).

4. Dependence on Cloud Location and Thickness

In order to illustrate the dependence of reflection and atmospheric absorption with respect to cloud location, we consider the nominal water vapor case and consider 100 mbar thick clouds located successively at 200–300, 500–600, and 800–900 mbar, all having the same drop optical properties. The altitude variation effectively alters the water vapor content above the cloud and also that within the cloud layer (owing to the differences in vapor mixing ratio and saturation values prevailing at different altitudes) [see, e.g., *Davies et al.*, 1984; *Chou*, 1989; *Schmetz*, 1993; RF98]. Figure 3 displays the results of the computations. Cloud location affects both albedo and absorption. The cloud at 300 mbar reflects the most solar radiation but absorbs the least of the three systems considered. The latter is attributable principally to the diminished role of the above-cloud water vapor for this case. The atmospheric absorption varies considerably with cloud location and comprises changes due to the amount of vapor present above the cloud as well as the saturated amount present in the cloud, with both factors enhancing the absorption the lower the cloud. The pattern of the total solar spectrum results is similar to that found when only the near-IR spectrum is considered (RF98). The net TOA irradiance decreases with increasing LWP and is monotonic with respect to cloud location. In contrast to Figures 1 and 2, however, Figure 3 shows that the net solar spectrum irradiance at the surface, given a nominal amount of vapor in the atmosphere, is insensitive to where the 100 mbar thick clouds are placed and depends only on LWP and r_{eff}. Therefore the TOA-to-surface irradiance ratio is, in general, an ambiguous one not only for the near infrared (RF98) but also when the total solar spectrum irradiance is considered.

Figure 4 shows a similar sensitivity corresponding to variations in r_{eff}, with LWP fixed at 500 g/m^2. The atmospheric albedo and absorption features again reveal a dependence on cloud height. The sensitivity of each parameter with respect to r_{eff} is almost similar no matter where the cloud is placed. As in Figure 3, the net TOA irradiance is sensitive to cloud height, but this is not so for the surface flux at any r_{eff}. There is a general linearity of the results with r_{eff} in contrast to the situation with LWP, owing to the reason mentioned above in the discussions concerning Figure 2.

Figure 5 shows the atmospheric reflection and absorption when clouds with varying geometric thicknesses are successively placed at various altitudes in the atmosphere. The cloud base is fixed at 900 mbar, while the top is varied from 880 mbar progressively up to 180 mbar. Thus the effective geometric thickness variation ranges from 20 to 720 mbar. The cloud LWP considered is 500 g/m^2, $r_{\text{eff}} = 10$ μm, and the resulting drop extinction optical depth is equal to 150. Water vapor is at saturation values in the cloud layers. As the geometric depth increases, the in-cloud vapor content increases but the above-cloud vapor path decreases. The latter acts to decrease the role of the above-cloud vapor absorption, and thus the reflection increases. The results indicate a general monotonic, near-linear relationship for the absorption and albedo, with distinctly different values for different pressure thicknesses. The results also reiterate the importance of the location of cloud top, which determines the amount of absorption by the above-cloud water vapor [e.g., *Schmetz*, 1993; RF98]. For the cloud characteristics considered, there is very little irradiance at the surface (not shown), but it is nevertheless approximately the same with respect to cloud location (range 49–59 W/m^2), and

approximately consistent with Figures 3 and 4. In contrast, the net TOA irradiance varies by ~100 W/m^2 for the range in geometric thickness considered. For the present considerations the net TOA-to-surface irradiance ratio varies from ~442/57 (i.e., 7.8) for the 20 mbar geometric thickness case to ~325/49 (i.e., 6.7) for the 720 mbar thickness case, thus indicating a sensitivity of ~15% to fairly extreme changes in cloud top and geometric depth, with the drop characteristics held fixed.

5. Optically Thick Cloud

We explore next the asymptotic limit attained when clouds of infinite drop extinction optical depths are considered. We assume that the "infinite" nature is due to the occurrence of very large LWPs. To obtain the reflection and absorption by such clouds, we follow the formulation of *Wiscombe and Warren* [1980] and *Chylek et al.* [1983]. The radiative properties of such clouds would depend on the single-scattering albedo and, to a lesser extent, the asymmetry factor of the cloud layer. These parameters are determined both by the drop size considered and, to a lesser extent, by the amount of water vapor present in the layer. It would also depend on the amount of water vapor above the cloud and thus on the cloud location [*Chou*, 1989; *Schmetz*, 1993].

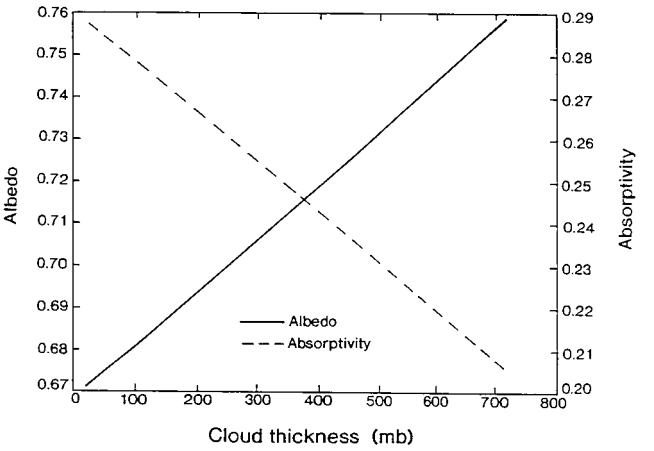

Figure 5. Albedo and atmospheric absorptivity as a function of cloud geometric thickness. Cloud LWP is 500 g/m^2 and r_{eff} = 10 μm. The variation of geometric thickness is accomplished by fixing the cloud base at 900 mbar and moving the top progressively from 880 to 180 mbar (see section 4).

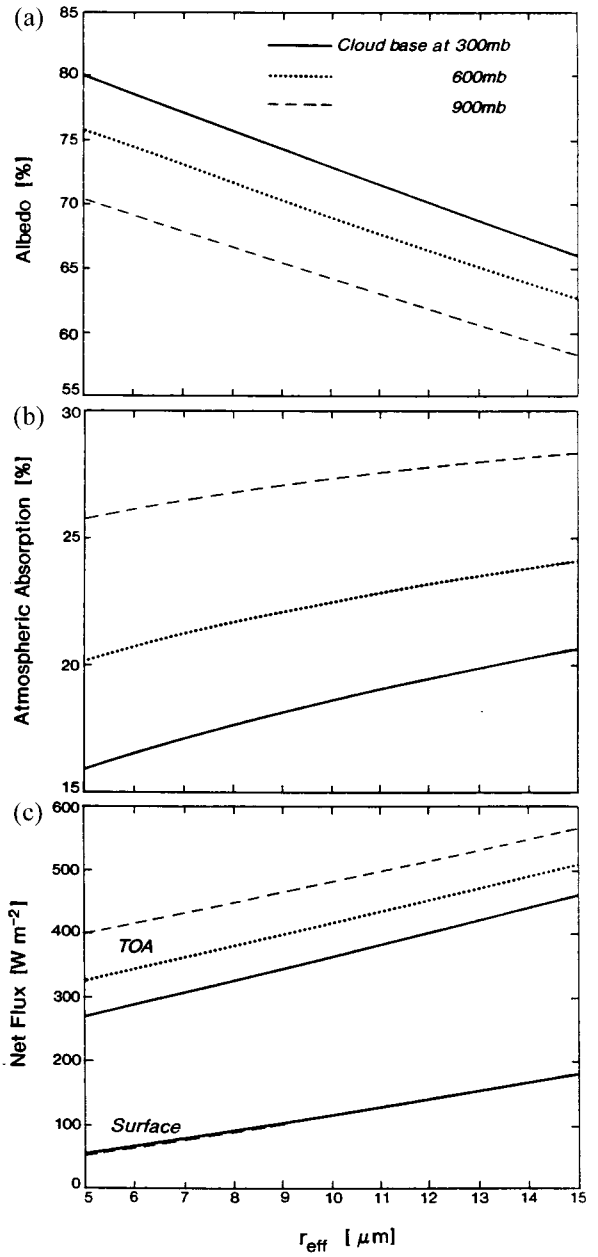

Figure 4. Same as Figure 3, except plotted as a function of r_{eff}, and with LWP held fixed at 500 g/m^2.

We consider a cloud located at 800–900 mbar and, first, assume nominal atmospheric water vapor conditions. The value of the computed albedo for such a cloud varies from 0.74 for r_{eff} = 5 μm, to 0.72 for r_{eff} = 10 μm, to 0.70 for r_{eff} = 15 μm, while the atmospheric absorption increases from 0.25 to 0.28 to 0.30, respectively. Since the single-scattering co-albedo increases in the near infrared with size, hence a larger r_{eff} yields greater absorptivity. Thus r_{eff} is an important determinant of the asymptotic limit of absorption for very thick clouds; the effect on reflection is substantially less. The value for r_{eff} = 10 μm may be compared with the value at 1000 g/m^2 (nominal case curve) in Figure 1, which is the largest LWP considered in that figure. The value in Figure 1 is almost close to the limiting value derived using the analytic expressions.

Next we compare the effects between the nominal atmospheric water vapor assumption and the dry (atmosphere and cloud layers) case (see section 2) for a cloud with r_{eff} = 10 μm. Different asymptotic limits result for the albedo and atmospheric absorption. The effect of water vapor is seen to alter the albedo by 0.07, i.e., from 0.72 for the nominal case to 0.79 for the dry case. The increase in reflection is due to a greater amount of radiation incident on the cloud in the near absence of the above- and in-cloud vapor. In the case of atmospheric absorption, the alteration is from ~0.28 to 0.21, i.e., a ~33% effect enhancement occurs due to the presence of the nominal water vapor. The dry case, although having more radiation incident on the cloud, experiences less atmospheric absorption owing to lack of above- and in-cloud vapor. The nominal case has some absorption occurring above the cloud; further, the water vapor in the cloud makes an additional contribution, since there is now an increased absorption optical depth within the cloud layer compared to the drier case. Thus water vapor

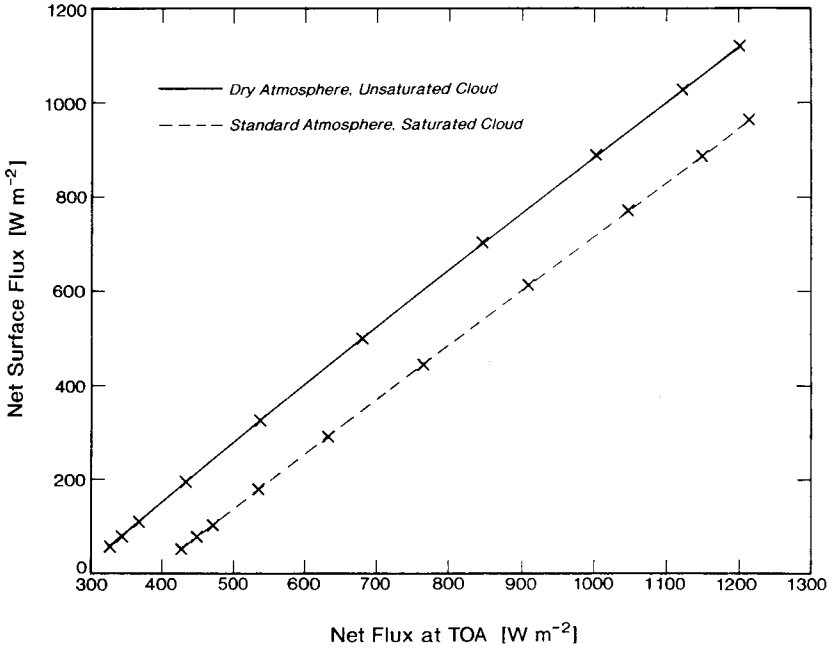

Figure 6. Net flux at surface versus that at TOA for two different assumptions concerning atmospheric water vapor (see section 6).

can play a nonnegligible role in atmospheric absorption even when clouds with very large LWPs are considered. Taken together with the results from section 4, cloud top location and atmospheric water vapor are of critical importance in determining atmospheric absorption.

6. Relation Between Net Fluxes at Top and Surface

Figures 1–5 reveal that the variations of the net solar irradiance at TOA and surface with respect to cloud characteristics and location are different from each other. An important point arising as a consequence concerns the relationship between the net TOA and surface irradiances. It is to be noted that most of the incoming solar flux is absorbed at the surface [e.g., *Kiehl and Trenberth*, 1997], with usually a lesser but significant amount absorbed in the atmosphere. Since the surface solar irradiance is an important component in the surface heat and moisture balance [e.g., *Chen and Ramaswamy*, 1995], there have been intensive efforts to estimate this by using satellite observations of the TOA net solar irradiance and some transformation function that relates the TOA irradiance to the surface irradiance in a simple manner [e.g., *Cess and Vulis*, 1989; *Schmetz*, 1993; *Li et al*., 1997]. Obviously, the great advantage is that, then, global surface shortwave radiative flux would become easily estimated from routine satellite measurements. Because net TOA irradiance represents the atmosphere+surface absorption while the net surface irradiance represents the surface absorption, the construction of a linear relation between these two quantities leads to a measure of the atmospheric absorption. Such a relation is indeed found to be quite generally valid in different types of clear skies [e.g., *Cess et al*., 1991; *Schmetz*, 1993]. However, as pointed out by RF98, based on rigorous calculations, such a relationship is not valid for arbitrary overcast atmospheres in the near-IR spectrum. Here we explore this issue further by considering the total solar spectrum irradiance in overcast skies, using again the idealized cloud cases of sections 2–4.

Using the 800–900 mbar cloud, different LWPs, $r_{\text{eff}} = 10$ μm, and the nominal and dry case water vapor conditions, we illustrate in Figure 6 a plot of the resulting net surface versus TOA irradiance relation. For any atmospheric water vapor condition assumed, there occurs a linear relation whose slopes and intercepts are listed in Table 1. The "dry" case has a slightly larger slope than the nominal one (by ~5%), indicating a higher sensitivity of the TOA-surface relation. This occurs because water vapor in the atmosphere acts to dampen the sensitivity of atmospheric absorptivity to LWP changes by saturating to a greater extent the near-infrared spectral absorption before it can reach the cloud. For the same net flux at the surface, the net TOA irradiance (comprising the surface plus atmospheric absorption) is greater for the nominal case, highlighting the importance of atmospheric water vapor in estimates of the atmosphere+surface absorption.

The numerical differences in TOA and surface irradiances between the nominal and dry environments at three different optical depths are listed in Table 2. At small optical depths the difference is more marked for the irradiance at the surface than at the top. In this limit, water vapor is a significant factor for the radiation reaching the surface, consistent with Figure 1c. At large optical depths it is the net TOA irradiance that is

Table 1. Regression Equations Relating the Surface and the TOA Net Irradiances (See Figure 6)

	S_{sfc}
Nominal case	$S_{\text{TOA}} \times 1.161–446.2$
Dry case	$S_{\text{TOA}} \times 1.219–335.1$

Two different assumptions are made concerning the atmospheric water vapor amount (see section 6). The relations are valid for the range shown in Figure 6. Units are W/m^2.

Table 2. Change in Surface (S_{sfc}) and Top (S_{TOA}) Irradiances Between the Dry Atmosphere and Nominal Water Vapor Case at Different Values of the Drop Extinction Optical Depth

Optical Depth	δS_{TOA}, W/m^2	δS_{sfc}, W/m^2
1.5	−20	+100
15	−83	+35
150	−100	+5

See section 6.

Table 3. Regression Equations Relating the Net Surface and TOA Irradiances (see Figure 7)

	S_{sfc}
Standard case	$S_{TOA} \times 1.161–446.2$
Altitude change	$S_{TOA} \times 1.076–334.1$
Geometric depth change	$S_{TOA} \times 1.012–288.2$
Sun angle change	$S_{TOA} \times 1.119–247.8$
Surface albedo	$S_{TOA} \times 1.142–441.5$

The standard case is with nominal water vapor amounts, cloud located at 800–900 mbar, r_{eff} = 10 μm, surface albedo of 0, and overhead Sun conditions. Other cases involve changes in one parameter at a time. The changes are altitude (cloud at 500–600 mbar), geometric depth (cloud at 180–900 mbar), Sun angle (53°), and surface albedo (0.8). The plot is constructed by performing calculations at several different LWPs for each of the aforementioned cases (see section 6). The relations are valid for the range shown in Figure 7. Units are in W/m^2.

affected more as atmospheric absorption is dominated by the drops, and assumptions about vapor conditions affect drop radiative interactions. Note that, for moderate optical depths (e.g., 15), the differences in both the surface and atmospheric absorption irradiances caused by water vapor remain considerable.

Figure 7 generalizes the sensitivity of the TOA-surface relation to various factors, viz., geometric depth, vertical location, different Sun angles, and surface albedo. As far as water vapor is concerned, changes in the first two factors alter the above-cloud and in-cloud vapor amounts, while the solar zenith angle affects the water vapor path that has to be traversed before the beam reaches the cloud top. Surface albedo governs the multiple reflections between clouds and surface, potentially enhancing the in-cloud and atmospheric absorption, especially for optically thinner clouds. We perform this sensitivity study by considering the 800–900 mbar cloud with nominal water vapor (i.e., saturated vapor in cloud), r_{eff} = 10 μm, overhead Sun conditions, and zero surface albedo. We designate these as standard values. We consider several LWPs (10, 17.8, 31.6, 56.2, 100, 178, 316, 562, 750, and 1000 g/m^2; i.e., 10 different LWPs) to construct the "standard" case curve of the TOA-surface irradiance relationship in Figure 7. We then vary each of the four parameters, one at a time, and repeat the calculations for the same LWPs as above. In considering these variations, we choose values of the concerned parameters that represent a substantial departure from the standard case. Thus, for altitude variation, we consider the cloud to be between 500 and 600 mbar; for geometric depth variation, we consider a cloud extending from 180 to 900 mbar (this also implies an elevation of the cloud top); for Sun angle variation, we consider 53°; and for surface albedo variation, we consider a value of 0.8. The resulting net TOA and surface irradiances for each of the variations are also plotted in Figure 7. In the case of surface albedo variation, the results for the lowest three LWPs are discarded and not plotted. Table 3 lists the slope and

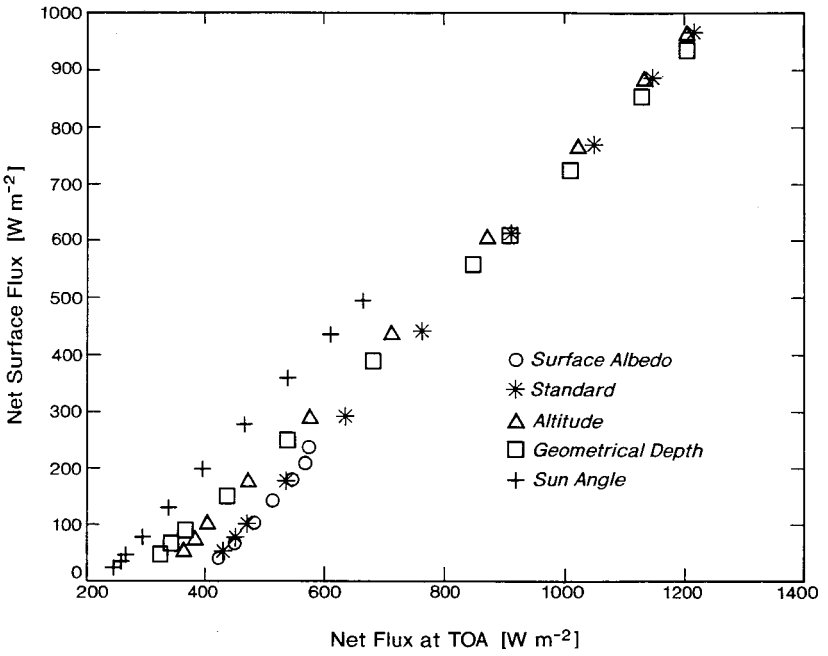

Figure 7. Net flux at surface versus that at TOA for different conditions. For any set of plotted points, different LWPs (fixed r_{eff}) are considered. Each set of plotted points represents variation in the value of one variable with respect to the standard case (see section 6). The values of the parameters varied with respect to the standard set of values are listed in Table 3.

intercept for the standard case as well as the corresponding values for each of the variations considered.

In general, each of the parameter variations as considered here yields a departure in the slope of the TOA-surface relationship. This is consistent with the findings of *Chou* [1989], *Li et al*. [1993], and *Masuda et al*. [1995]. The changes in the slope (up to ~15%) indicate that an increase of cloud altitude, geometric depth, surface albedo, and zenith angle with respect to the standard case modulates the sensitivity of the TOA-surface relationship, as investigated here for different LWPs. The departure of the intercept from the standard case is most when the Sun angle variation is considered, followed by geometric depth and then altitude variations, with surface albedo effect being only slightly different. Although the TOA-surface irradiance relation, with only one parameter varying at a time, remains linear, the nature of the linearity differs from that in the standard case.

A higher zenith angle means less irradiance. At the same time, there is a larger optical path traversed by the incident beam before it is incident on the cloud. Consequently, both TOA and surface irradiances are reduced for any LWP relative to the standard case. The slope is less than that for the standard case; this is consistent with the finding for the near-IR irradiance (RF98). The intercept is less in magnitude because of the lesser irradiance available; the magnitude is the least among the various factors considered here.

An increase of geometric depth results in a lesser sensitivity of the TOA-surface relation (i.e., smaller slope), as does the increase in the cloud altitude. Note that, at smaller LWPs (upper right section of the plot in Figure 7), the differences in the values for the standard case and for the altitude and geometric depth variation cases are relatively less; the TOA-surface relationship (a measure of atmospheric absorption) at relatively small drop optical depths is approximately similar for these circumstances.

As seen from section 4, an increase in cloud altitude keeping LWP fixed does not alter the surface irradiance. With the 500–600 mbar cloud reflecting more radiation, there is less atmospheric absorption and hence a lesser net TOA irradiance, while the transmission to the surface is nearly unchanged. Thus the slope, considering the entire range of LWP values, is less steep than in the standard case. The effect of the cloud location would be felt more for larger LWPs (Figure 3), and this is manifest in the lower left domain of Figure 7 when there are appreciable differences from the standard case values.

An increase in geometric depth of cloud coupled with an elevation of the cloud top (viz., 180–900 mbar cloud case) implies two things. One, there is more vapor inside cloud that would contribute to more absorption. However, there would also be more radiation reflected, since the vapor above cloud top is now reduced. Thus, while surface irradiance is affected only to a small extent, there is a reduction in the net TOA irradiance; this is more so when larger LWPs are considered. In fact, the sensitivity is even less (i.e., slope has a smaller value) than in the case when the cloud altitude alone is varied.

Compared to the standard case, the surface albedo influence is relatively less than that of the other factors in affecting the TOA-surface relationship, in terms of both the intercept and slope. However, it should be noted that when LWP is relatively small the surface and TOA values depart considerably from those in the standard case.

7. Conclusions

Water vapor in the atmosphere has a significant bearing on the reflection and absorption characteristics of cloudy atmospheres. Relative to a completely dry atmosphere, the presence of nominal water vapor, including saturated amounts within cloud layers, enhances the overcast sky absorption. Thus both theoretical and observational studies need to account for the atmospheric water vapor accurately, particularly in resolving the issue of solar absorption in overcast atmospheres. This involves necessarily precise estimates of the cloud top location as well as its geometric extent, even for the simple plane-parallel, homogeneous cases. These dependences are quite apart from the well-known ones on drop microphysical properties (LWP and r_{eff}). Even for optically thick clouds, the effective radius and water vapor amount are important factors in the degree of absorption. This study substantiates the earlier studies of *Chou* [1989] and *Schmetz* [1993] and adds to the high-resolution near-infrared calculations of *Crisp* [1997] and RF98. The sensitivity to the above factors is manifest in the TOA-surface irradiance relationships, thus adding to the study of *Cess et al*. [1991] and *Masuda et al*. [1995]. The nominal water vapor in the atmosphere lends a different sensitivity than an otherwise dry atmosphere. Dependence on both drop and vapor characteristics results in differing sensitivities of the TOA-to-surface irradiance relationship for different types of clouds, such as low versus middle clouds, geometrically moderate versus very thick clouds. There also arise differing sensitivities for different zenith angles. The sensitivities clearly indicate that, in general, TOA irradiances cannot unambiguously yield the surface irradiance or the atmospheric absorption in cloudy skies without additional information on the factors mentioned above. This is especially so when quantitative estimates to a high degree of accuracy are required for evaluations against climatological observations, and for determining climate variations and change. While the inference in this study is based on plane-parallel, horizontally homogeneous clouds, it would be of interest to examine whether the conclusion reached here breaks down for the case of broken clouds or partly cloudy skies.

Acknowledgments. We thank S. M. Freidenreich for help with the use of the model and for comments on the manuscript. Support for K. K. Fung's tenure in the AOS Summer Student Program by NOAA is gratefully acknowledged. Comments by two anonymous referees proved very helpful.

References

Briegleb, B., Delta-Eddington approximation in the NCAR Community Climate Model, *J. Geophys. Res*., *97*, 7603–7612, 1992.

Cess, R. D., and I. L. Vulis, Inferring surface solar absorption from broadband satellite measurements, *J. Clim*., *2*, 974–985, 1989.

Cess, R. D., E. G. Dutton, J. J. DeLuisi, and F. Jiang, Determining solar absorption from broadband satellite measurements for clear skies: Comparison with surface measurements, *J. Clim*., *4*, 236–247, 1991.

Chen, C.-T., and V. Ramaswamy, Parameterization of the solar radiative characteristics of low clouds and studies with a general circulation model, *J. Geophys. Res*., *100*, 11,611–11,622, 1995.

Chou, M.-D., On the estimation of surface radiation using satellite data, *Theor. Appl. Climatol*., *40*., 25–36, 1989.

Chylek, P., V. Ramaswamy, and V. Srivastava, Albedo of soot-contaminated snow, *J. Geophys. Res*., *88*, 10,837–10,843, 1983.

Crisp, D., Absorption of sunlight by water vapor in cloudy conditions: A partial explanation for the cloud absorption anomaly, *Geophys. Res. Lett*., *24*, 571–574, 1997.

Davies, R., W. L. Ridgway, and K.-E. Kim, Spectral absorption of solar radiation in cloudy atmospheres: A 20 cm^{-1} model, *J. Atmos. Sci*., *41*, 2126–2137, 1984.

Freidenreich, S. M., and V. Ramaswamy, A new multiple-band solar radiative parameterization for general circulation models, *J. Geophys. Res*., in press, 1999.

Joseph, J. H., W. Wiscombe, and J. A. Weinman, The delta-Eddington approximation for radiative flux transfer, *J. Atmos. Sci*., *33*, 2452–2459, 1976.

Kiehl, J. T., and K. E. Trenberth, Earth's annual global mean energy budget, *Bull. Am. Meteorol. Soc*., *78*, 197–208, 1997.

Li, Z., H. G. Leighton, K. Masuda, and T. Takashima, Estimation of SW flux absorbed at the surface from TOA reflected flux, *J. Clim*., *6*, 317–330, 1993.

Li, Z., L. Moreau, and A. Arking, On solar energy disposition: A perspective from observation and modeling, *Bull. Am. Meteorol. Soc*., *78*, 53–70, 1997.

Masuda, K., H. G. Leighton, and Z. Li, A new parameterization for the determination of solar flux absorbed at the surface from satellite measurements, *J. Clim*., *8*, 1615–1629, 1995.

McClatchey, R. A., R. W. Fenn, J. E. A. Selby, F. E. Volz, and J. S. Garing, Optical Properties of the Atmosphere, *Rep. AFCRL-72-0497*, 110 pp., Hanscom Air Force Base, Bedford, Mass., 1972.

Ramaswamy, V., and M. M. Bowen, Effects of changes in radiatively active species upon the lower stratospheric temperatures, *J. Geophys. Res*., *99*, 18,909–18,921, 1994.

Ramaswamy, V., and S. M. Freidenreich, Solar radiative line-by-line determination of water vapor absorption and water cloud extinction in inhomogeneous atmospheres, *J. Geophys. Res*., *96*, 9133–9157, 1991.

Ramaswamy, V., and S. M. Freidenreich, A high-spectral resolution study of the near-infrared solar flux disposition in clear and overcast atmospheres, *J. Geophys. Res*., *103*, 23,255–23,273, 1998.

Schmetz, J., Relationship between solar net radiative fluxes at the top of the atmosphere and at the surface, *J. Atmos. Sci*., *50*, 1122–1132, 1993.

Slingo, A., A GCM parameterization for the shortwave radiative properties of water clouds, *J. Atmos. Sci*., *46*, 1419–1427, 1989.

Stephens, G. L., Radiation profiles in extended clouds, I, Theory, *J. Atmos. Sci*., *35*, 2111–2122, 1978.

Wiscombe, W., and S. Warren, A model for the spectral albedo of snow, I, Pure snow, *J. Atmos. Sci*., *37*, 2712–2733, 1980.

K. K. Fung and V. Ramaswamy, NOAA GFDL, Princeton University, P. O. Box 308, Princeton, NJ 08542.

(Received January 29, 1999; revised June 8, 1999;
accepted June 15, 1999.)